

1 **Author response to Editor**

19 March 2015

2

3

4 Manuscript no. hess-2014-268, "Estimation of temporal and spatial variations in groundwater  
5 recharge in unconfined sand aquifers using Scots pine inventories" by Ala-aho, P. et al.

6

7 Dear Editor Dr. Stumpp,

8 Thank you for the positive feedback regarding the modifications made in the manuscript.  
9 Remaining two recommendations for improvement by you and reviewer A. Basile are  
10 acknowledged and changes in the manuscript are made as specified below.

11

12 Sincerely,

13 Pertti Ala-aho

14 Water resources and environmental engineering research group  
15 University of Oulu

16

17

18 **Editor comments:**

19 Improvement is needed for "soil" terminology and information about the lichen layer. I totally  
20 agree to reviewer #2's comment on the terminology of "soil" and would appreciate if you place  
21 the terms correctly into your manuscript rather than using the broad definition for soil.

22

23 **Point #1**

24 *The first is a technical point. It still was not clear to me the parameterization of the lichens  
25 layer. I already ask you an answer on this topic but I didn't find any answer to this point.*

26 *In rows 186-188 of the new manuscript you stated " The mean water retention capacity of the  
27 lichen samples was found to be 9.85 mm (standard deviation (SD) 2.71 mm) and  
28 approximations for these values were used in model parameterization (Table 2)."*

29 *You've expressed such result in mm, but in table 2 you've reported the porosity  $\theta_L$  as %. The  
30 latter seems to me correct. The porosity is generally an a-dimensional parameter, and  
31 specifically is a-dimensional in the B&C equation.*

32 *I wonder that a confusion was made between the results of the water storage coming from the  
33 experiment (i.e. 9.85 mm) and the parameter you have to apply.*

34 *Please clarify this point.*

35

36 Thank you for this valuable comment. Explanation of this was only included as a comment in  
37 the annotated manuscript, but unjustifiably left out of the manuscript revision. Detailed  
38 description of the lichen parametrization is added to the (final) manuscript on lines 191-196.  
39 Also discussion on the topic is slightly modified on lines 564-566.

40

41 **Point #2**

42 *The second point is more general and do not pertain only to this paper. I'm using the revision*

43 *of this paper and the open-discussion as an opportunity to remark a crucial point.*

44 *In rows 113-114 of the new manuscript and in your answers you stated "Rokua is an*

45 *unconfined, aquifer consisting of unconsolidated sandy sediments (from here on referred to as*

46 *soil)". In such a way any possible misunderstanding in the paper reading is avoided.*

47 *Formally, everything is ok. The authors have answered to the question I posed in the first*

48 *revision.*

49 *...BUT...*

50 *...a more general question arise...*

51 *I've not teaching you that the soil is something more complex of an "unconsolidated sandy*

52 *sediment". I know that in your scientific community is often usual to call soil any porous*

53 *material under earth surface. But, I think this is wrong and not correct, especially for a*

54 *multidisciplinary and interdisciplinary journal. I think that we have to produce many efforts*

55 *to overcome this "cultural" problem that many scientific communities suffer (including soil*

56 *scientist in general and me in particular). Interdisciplinarity is a powerful concept but*

57 *sometimes...just a concept. We have to do any effort to translate it in real facts and not just*

58 *use it as slogan or empty words. Specifically, the soil (that is a very complex – and hidden -*

59 *resource) is neglected in too hydrology-related papers. But this complexity should be fuel for*

60 *us to go on and try to manage it and not a wall to turn around.*

61

62 This is a good point of discussion as sometimes all porous geological material is referred to as

63 soil in hydrogeological literature. This can be confusing, and in this work terminology is

64 revised. When referring to the 1-D porous media column for which water flow is simulated,

65 term "soil" is replaced with "sediment". Changes can be seen throughout the manuscript text,

66 in Table 2, and in Figs. 1, 2, and 5

67

68

69

70

71

72

73

74

75 **Estimation of temporal and spatial variations in**  
76 **groundwater recharge in unconfined sand aquifers using**  
77 **Scots pine inventories**

78

79 **P. Ala-aho<sup>1</sup>, P.M. Rossi<sup>1</sup> and B. Kløve<sup>1</sup>**

80

81 [1] Water Resources and Environmental Engineering Research Group, Faculty of Technology,  
82 University of Oulu, P.O. Box 4300, 90014 University of Oulu, Finland

83 Correspondence to: P. Ala-aho (perti.ala-aho@oulu.fi)

84

85

86

87

88

89

90

91

92

93

94

95

96

97

98

99

100 **Abstract**

101 Climate change and land use are rapidly changing the amount and temporal distribution of  
102 recharge in northern aquifers. This paper presents a novel method for distributing Monte Carlo  
103 simulations of 1-D ~~soil~~ sandy sediment profile spatially to estimate transient recharge in an  
104 unconfined esker aquifer. The modeling approach uses data-based estimates for the most  
105 important parameters controlling the total amount (canopy cover) and timing (thickness of the  
106 unsaturated zone) of groundwater recharge. Scots pine canopy was parameterized to leaf area  
107 index (LAI) using forestry inventory data. Uncertainty in the parameters controlling ~~soil~~  
108 sediment hydraulic properties and evapotranspiration was carried over from the Monte Carlo  
109 runs to the final recharge estimates. Different mechanisms for lake, soil, and snow evaporation  
110 and transpiration were used in the model set-up. Finally, the model output was validated with  
111 independent recharge estimates using the water table fluctuation method and baseflow  
112 estimation. The results indicated that LAI is important in controlling total recharge amount.  
113 Soil evaporation compensated for transpiration for areas with low LAI values, which may be  
114 significant in optimal management of forestry and recharge. Different forest management  
115 scenarios tested with the model showed differences in annual recharge of up to 100 mm. The  
116 uncertainty in recharge estimates arising from the simulation parameters was lower than the  
117 interannual variation caused by climate conditions. It proved important to take unsaturated  
118 thickness and vegetation cover into account when estimating spatially and temporally  
119 distributed recharge in sandy unconfined aquifers.

120

121

122

123

124

125

126

127

128

129 **1 Introduction**

130 Eskers are permeable, unconfined sand and gravel aquifers (Banerjee, 1975). In addition to  
131 water supply, they support groundwater-dependent ecosystems and provide recreational  
132 services (Kløve et al., 2011). Esker hydrology is important as eskers and other glaciofluvial  
133 aquifer types cover large areas of the North and are among the dominant aquifer types in the  
134 boreal zone. Management of these complex aquifers has gained recent attention (Bolduc et al.,  
135 2005, Karjalainen et al., 2013, Koundouri et al., 2012, Kurki et al., 2013). The European  
136 Groundwater Directive requires such systems to be characterized in order to determine their  
137 quality status, so knowledge of how to estimate groundwater recharge in esker aquifers is  
138 becoming increasingly important (EC, 2006). Esker aquifers are commonly covered with  
139 managed pine forests, where the forest canopy is likely to influence recharge amounts. The soil  
140 surface profile of eskers is complex and highly variable, consisting of kettle holes and sand  
141 dunes, resulting in variable thickness of the unsaturated zone (Aartolahti, 1973), a factor which  
142 also needs to be accounted for in recharge estimation.

143 Computational methods to estimate groundwater recharge vary from simple water balance  
144 models, where water stores and fluxes are represented conceptually and related with adjustable  
145 parameters (Jyrkama et al., 2002), to physically-based models using the Richards equation  
146 (Assefa and Woodbury, 2013, Okkonen and Kløve, 2011) to solve water fluxes through  
147 unsaturated zone. Computational methods solving the Richards equation are often limited to  
148 small-scale areal simulations (Scanlon et al., 2002a) and shallow unsaturated zones, and they  
149 commonly lack the soil freeze, thaw, and snow storage sub-routines relevant at higher northerly  
150 latitudes (Okkonen, 2011). However, computational approaches can be employed to produce  
151 the values on spatial and temporal variability in recharge often needed in groundwater modeling  
152 (Dripps and Bradbury, 2010). The methods commonly rely on a GIS platform for spatial  
153 representation and calculation approaches based on water balance to create the temporal  
154 dimension of recharge (Croteau et al., 2010, Dripps and Bradbury, 2007, Jyrkama et al., 2002,  
155 Sophocleous, 2000, Westenbroeck et al., 2010). Neglecting variations in thickness of the  
156 unsaturated zone is common practice in many water balance models used in recharge  
157 estimations. However, the residence time in the unsaturated zone may play an important role,  
158 especially in the timing of recharge in deep unsaturated zones (Hunt et al., 2008), as  
159 acknowledged in recent work (Assefa and Woodbury, 2013, Jyrkama and Sykes, 2007, Scibek  
160 and Allen, 2006, Smerdon et al., 2008).

161 In numerical recharge models, actual evapotranspiration (ET) is a difficult variable to estimate  
162 accurately from climate, soil, and land use data. The vegetation is commonly parameterized  
163 from land use or land cover maps (Assefa and Woodbury, 2013, Jyrkama et al., 2002, Jyrkama  
164 and Sykes, 2007, Keese et al., 2005), where the vegetation characteristics and leaf area index  
165 (LAI) are estimated based solely on vegetation type. In addition to tree canopy transpiration,  
166 soil evaporation, i.e. evaporation from the pores of soil matrix, can constitute a large proportion  
167 of total ET. Soil evaporation from the forest floor is generally reported to range from 3 to 40%  
168 of total ET (Kelliher et al., 1993), although values as high as 92% have been recorded (Kelliher  
169 et al., 1998). For conifer forest canopies, soil evaporation can largely compensate for low  
170 transpiration in areas with lower LAI (Ohta et al., 2001, Vesala et al., 2005). Data on canopy-  
171 scale evaporation rates at latitudes above 60°N are rare (Kelliher et al., 1993). A few studies  
172 have estimated ET from pine tree stands at patch scale (Kelliher et al., 1998, Lindroth, 1985),  
173 but none has extended this analysis to spatially distributed groundwater recharge. Forest  
174 management practices have the potential to affect the transpiration characteristics of coniferous  
175 forests, which typically leads to increased groundwater recharge (Bent, 2001, Lagergren et al.,  
176 2008, Rothacher, 1970).

177 The overall aim of the study was to provide novel information on groundwater recharge rates  
178 and factors contributing to the amount, timing, and uncertainty of groundwater recharge in  
179 unconfined sandy eskers aquifers. Study expands the application of physically-based 1-D  
180 unsaturated water flow modeling for groundwater recharge, while taking into account detailed  
181 information on vegetation (pine, lichen), unsaturated layer thickness, cold climate, and  
182 simulation parameter uncertainty. Furthermore, this study considers the effect that forestry land  
183 use has on vegetation parameters and how this is reflected in groundwater recharge.

184

## 185 **2 Materials and Methods**

### 186 **2.1 Study site**

187 Groundwater recharge was estimated for the case of the Rokua esker aquifer in northern Finland  
188 (Fig. 1). Rokua is an unconfined aquifer consisting of unconsolidated sandy sediments (~~from~~  
189 ~~here on referred to as soil~~) underlain by crystalline bedrock (Fig. 2). Aquifer was formed  
190 during previous deglaciation when rivers under the melting ice sheet deposited sandy sediments  
191 in the river bed (Aartolahti 1973). The Rokua esker has a rolling surface topography in the

192 aquifer recharge area rising about 60 m above the flat peatland areas surrounding the esker. In  
193 the groundwater discharge areas, the aquifer is locally confined by peat soil with low hydraulic  
194 conductivity (Rossi et al. 2012).

195 The climate at the Rokua aquifer is characterized by precipitation exceeding evapotranspiration  
196 on an annual basis and statistics of the annual climate for the study period 1961 - 2010 in terms  
197 of precipitation, air temperature and FAO reference evapotranspiration according to Allen et al.  
198 (1998) is presented in Table 1. Another important feature of the climate is annually recurring  
199 winter periods when most precipitation is accumulated as snow.

### 200 2.1.1 Leaf area index from forestry inventories

201 Forestry inventory data from the Finnish Forest Administration (Metsähallitus, MH) and  
202 Finnish Forest Centre (Metsäkeskus, MK) were used to estimate LAI for the Rokua esker  
203 groundwater recharge area. The available data consisted of 2786 individual plots covering an  
204 area of 52.4 km<sup>2</sup> (62.4% of the model domain). The forestry inventories, performed mainly  
205 during 2000-2011, showed that Scots pine (*Pinus sylvestris*) is the dominant tree in the model  
206 area (94.2% of plots). The forest inventory data include a number of data attributes and the  
207 following data fields, included in both the MH and MK datasets, were used in the analysis:

- 208 - Plot area ( $p_A$ ); [ha]
- 209 - Main canopy type
- 210 - Average tree stand height ( $h$ ); [m]
- 211 - Average stand diameter at breast height ( $d_{bh}$ ); [cm]
- 212 - Number of stems ( $n_{stm}$ ); [ $1 \text{ ha}^{-1}$ ]
- 213 - Stand base area ( $b_A$ ); [ $\text{m}^2 \text{ ha}^{-1}$ ]
- 214 - Stand total volume ( $V$ ); [ $\text{m}^3$ ]

215 Inventory plots were excluded from the analysis if: (1) main canopy type was not pine forest,  
216 (2) data were missing for  $d_{bh}$  and  $h$  or  $n_{stm}$ , or (3) the MH and MK datasets overlapped, in which  
217 case MH was retained. However, several plots in the MH dataset were lacking  $n_{stm}$  data, which  
218 would have created a large gap in data coverage. Therefore the  $n_{stm}$  variable was estimated with  
219 a log-transformed regression equation using data on  $d_{bh}$ ,  $p_A$ , and  $V$  as independent variables.  
220 This regression equation was built from 280 plots ( $R^2 = 0.88$ ) and used to estimate  $n_{stm}$  for 288

221 plots. LAI was estimated as described by Koivusalo et al. (2008). Needle mass for an average  
222 tree in stand/plot was estimated from  $h$  and  $d_{bh}$  using empirical equations presented by Repola  
223 et al. (2007). LAI for a stand was calculated as:

$$224 \quad LAI = N_t * n_{stm} * S_{LA} \quad (1)$$

225 where  $N_t$  = needle mass per average tree in stand [kg],  $n_{stm}$  = number of stems per hectare  
226 [ $1 \text{ ha}^{-1}$ ], and  $S_{LA}$  = specific leaf area =  $4.43 \text{ m}^2 \text{ kg}^{-1} = 4.43 * 10^{-4} \text{ ha kg}^{-1}$  (Xiao et al., 2006).

227 Detailed information on LAI was used to obtain an estimate of how different forest management  
228 options, already actively in operation in the area, could potentially affect groundwater recharge.  
229 Three scenarios were simulated testing the potential impact of forestry operations on  
230 groundwater recharge:

- 231 1) The first “baseline” scenario simulated the current situation by using LAI pattern at  
232 the site (Fig. 3) estimated with Eq. (1).
- 233 2) The second scenario simulated the impact of intensive forestry operations as clear-  
234 cutting of the tree stand. Clear-cutting is an intensive land use form where almost the  
235 entire tree stand is removed, and it is carried out in some parts of the study area. Low  
236 LAI values of 0-0.2 for the whole study site were used in simulating this scenario.
- 237 3) The third scenario simulated the impact of no forestry operations, i.e. absence of  
238 forestry cuttings. The hypothetical mature stand covering the study site was assumed  
239 to have high LAI values of 3.2-3.5 found at the study site and reported in the literature  
240 (Koivusalo et al., 2008, Rautiainen et al., 2012, Vincke and Thiry, 2008, Wang et al.,  
241 2004).

## 242 2.1.2 Lichen water retention

243 An organic lichen layer covers much of the sandy soil at the Rokua study site (Kumpula et al.,  
244 2000), so this lichen layer was introduced in soil evaporation (SE) calculations. Although  
245 lichens do not transpire water, their structural properties allow water storage in the lichen matrix  
246 and capillary water uptake from the soil (Blum, 1973, Larson, 1979). In this study, lichen layer  
247 was explicitly included in the simulations to create an additional storage for water before the



248 mineral sandy sediments. ~~w~~Water interception storage by the lichen layer was estimated from  
249 lichen samples. In total, six samples (species *Cladonia stellaris* and *C. rangiferina*) were taken  
250 in May 2011 from two locations 500 m apart, close to borehole MEA506 (see Fig. 1). These  
251 samples were collected by pressing plastic cylinders (diameter 10.6 cm) through the lichen layer  
252 and extracting intact cores, after which mineral soil was carefully removed from the base of the  
253 sample. Thus the final sample consisted of a lichen layer on top and a layer of organic litter and  
254 decomposed lichen at the bottom, and was sealed in a plastic bag for transportation. To obtain  
255 estimates of water retention capacity, the samples were first wetted until saturation with a  
256 sprinkler, left overnight at +4 °C to allow gravitational drainage and weighed to determine ‘field  
257 capacity’. The samples were then allowed to dry at room temperature and weighed daily until  
258 stable final weight (‘dry weight’) was reached. The water retention capacity ( $w_r$ ) of the sample  
259 was calculated as:

$$260 \quad w_r = \frac{m_{fc} - m_{dry}}{\rho_w} \cdot \frac{1}{\pi \cdot r^2} \quad (2)$$

261 where  $m_{fc}$  is the field capacity weight [M],  $m_{dry}$  is the final dry weight [M] at room temperature,  
262  $\rho_w$  [M L<sup>-3</sup>] is the density of water, and  $r$  [L] is the radius of the sampling cylinder.

263 The mean water retention capacity of the lichen samples was found to be 9.85 mm (standard  
264 deviation (SD) 2.71 mm) and approximations for these values were used in model  
265 parameterization (Table 2). Measured lichen water retention capacity was introduced to the  
266 simulations using parameters for soil porosity and layer thickness. Lichen porosity values were  
267 varied between 7.5 - 12.5 % in simulation Monte Carlo runs (see section 2.2.1) while keeping  
268 thickness of the lichen layer at 100 mm. In this manner the maximum amount of water retained  
269 by the lichen layer after gravitational drainage was adjusted to vary between 7.5 mm - 12.5 mm.  
270 as seen in the measurement data. To acknowledge the lack of information about ~~(B&C)~~  
271 parameter estimates for lichen, the parameters were included in the simulations Monte Carlo  
272 runs (~~see section 2.2.1~~) with ranges which in our opinion produced reasonable shape of the  
273 pressure-saturation curve allowing easy drainage of the lichen.

### 274 2.1.3 ~~Soil~~ Sandy sediment hydraulic properties

275 ~~Soil~~ Sediment texture was determined by sieving (ISO 3310-1 standard sieve, US sieve numbers  
276 5, 10, 18, 35, 60, 120, and 230) -26 ~~soil~~ samples taken from five boreholes at various depths  
277 (Fig. 1). 14 of the samples were analyzed also for pressure saturation curves. Samples were  
278 characterized as fine or medium sand, while ~~soil~~ sediment texture in the other boreholes (Fig.

Commented [PA1]: Point#1; lichen parameterization explained in detail

279 1) had previously been characterized as medium, fine or silty sand throughout the model domain  
280 by the Finnish Environmental Administration as expert *in-situ* analysis during borehole drilling.  
281 Therefore the ~~soil~~-sediment samples from the five boreholes were considered to be  
282 representative of the ~~soil~~-sediment type in the area. Pressure saturation data from the samples  
283 was then used to define parameter ranges for the Brooks and Corey equation used in the  
284 simulations (Table 2). Furthermore, texture values were employed to calculate the range of  
285 saturated vertical hydraulic conductivity for the samples, using empirical equations by Hazen,  
286 Kozeny-Carman, Breyer, Slitcher, and Terzaghi (Odong, 2007). The hydraulic conductivity for  
287 a given sample ranged approximately one order of magnitude between the equations. When  
288 using the five equations for the 26 samples in total, the calculated values were within  $1.99 \cdot 10^{-5}$   
289  $- 1.47 \cdot 10^{-3} \text{ [m s}^{-1}\text{]}$  for all but one sample. The obtained range was considered to reasonably  
290 represent the hydraulic conductivity variability in the study area and simulations.

#### 291 2.1.4 Climate data

292 Driving climate data for the model were taken from Finnish Meteorological Institute databases  
293 for the modeling period 1 Jan 1961-31 Oct 2010. Daily mean temperature [°C] and sum of  
294 precipitation [mm] were recorded at Pelso climate station, 6 km south of the study area (Fig.  
295 1). The most representative long-term global radiation data [ $\text{kJ m}^{-2} \text{ d}^{-1}$ ] for the area were  
296 available as interpolated values in a 10 x 10 km grid covering the whole of Finland. The  
297 interpolation data point was found to be at approximately the same location as borehole  
298 MEA2110 (Fig. 1). Long-term data on wind speed [ $\text{m s}^{-1}$ ] and relative humidity [%] were taken  
299 from Oulunsalo and Kajaani airports, located 60 and 40 km from the study site, respectively.  
300 The data from the airports were instantaneous observations at three-hour intervals, from which  
301 daily mean values were calculated. All the climate variables were recorded at reference height  
302 2 m except for wind speed, which was measured at 10 m height. The wind speed data were  
303 therefore recalculated to correspond to 2 m measurement height according Allen et al. (1998)  
304 by multiplying daily average wind speed by 0.748. The suitability of long-term climate data for  
305 the study site conditions was verified with observations made at a climate station established at  
306 the study site in an overlapping time period (Dec 2009-Oct 2010) and the agreement between  
307 the measurements was found to be satisfactory.

308 Data on long-term lake surface water temperature were needed to calculate lake evaporation  
309 (see section 2.2.3), but were not available directly at the study site. However, surface water  
310 temperature was recorded at Lake Oulujärvi by the Finnish environmental administration

311 (2013) 22 km from the study site in the direction of the Kajaani climate station (Fig. 1). The  
312 Oulujärvi water temperature was found to be closely correlated (linear correlation coefficient  
313 0.97) with daily lake water temperature recorded at Rokua during summer 2012. Daily lake  
314 surface temperature data for Lake Oulujärvi starting from 21 July 1970 were used in lake  
315 evaporation modeling. However, the data series had missing values for early spring and some  
316 gaps during five years in the observation period. These missing values were estimated with a  
317 sine function, corresponding to the average annual lake temperature cycle, and a daily time  
318 series was established for subsequent calculations.

319 Snowmelt was calculated with a degree-day approach model in Jansson and Karlberg (2004).  
320 Snow routines were calibrated separately using bi-weekly snow water equivalent (SWE) data  
321 from Vaala snowline measurements (Finnish environment administration, 2011) for the period  
322 1960-2010 (Fig. 1). This separately calibrated snow model was used for all subsequent  
323 simulations.

## 324 **2.2 Recharge modeling framework**

### 325 2.2.1 Water flow simulation in 1-D unsaturated soil-sediment profile

326 Water flow through an unsaturated one-dimensional (1-D) sandy soil-sediment profile (Fig. 2)  
327 was estimated with the Richards equation using CoupModel (Jansson and Karlberg, 2004).  
328 CoupModel was selected as the simulation code because of its ability to represent the full soil-  
329 plant-atmosphere continuum adequately and to include snow processes in the simulations  
330 (Okkonen and Kløve, 2011). The simulated soil-sediment profile was vertically discretized into  
331 61 layers with increasing layer thickness deeper in the profile. Layer thickness was 0.1 m for  
332 the first 16 layers (until 1.6 m), where the topmost 0.1 m was represented as a lichen layer.  
333 Layer thickness was progressively increased by defining 0.2 m thickness for the next 7 layers  
334 (between 1.6 and 3 m), 0.5 m for the next 14 layers (between 3 and 10 m), 1 m for the next 7  
335 layers (between 10 and 17 m) and 2 m for last 17 layers ranging from 17 m to the bottom of the  
336 profile (51 m).

337 The time variable boundary condition for water flow at the top of the column was defined by  
338 driving climate variables and affected by sub-routines accounting for snow processes with daily  
339 time step. The short time step was chosen to fully capture the main recharge input from  
340 snowmelt. All water at the top of the domain was assumed to be subjected to infiltration. Deep  
341 percolation as gravitational drainage was allowed from soil-sediment column base using the

342 unit-gradient boundary condition (see e.g. Scanlon et al., 2002b). Simulations for the  
343 unsaturated 1-D soil-sediment profile were made for the period 1970-2010, and before each run  
344 10 years of data (1960-1970) were used to spin up the model.

345 The simulation of the 1-D soil-sediment profile was performed 400 times as Monte Carlo runs  
346 to facilitate the propagation of model parameter uncertainty in the final model output. Model  
347 was ran each time with different parameter values as specified in Table 2. For each individual  
348 simulation homogeneity in the vertical direction in terms of soil-sediment hydraulic properties  
349 was assumed. The parameters for which values were randomly varied were chosen beforehand  
350 by trial and error model runs exploring the sensitivity of parameters with respect to cumulative  
351 recharge or evapotranspiration. The parameter ranges were specified from field data when  
352 possible; otherwise we resorted to literature estimates or in some cases used  $\pm 50\%$  of the  
353 CoupModel default providing a typical parameter for the used equation.

354 The sensitivity of the parameters varied in the simulations was tested with Kendall correlation  
355 analysis, by testing the correlation between each model parameter and cumulative sums of  
356 different evapotranspiration components and soil-infiltration for the 400 model runs. Individual  
357 simulation with unique parameter values did not produce a groundwater recharge value due to  
358 the assembling strategy for recharge; therefore the ET components and soil-infiltration were  
359 selected as variables for comparison. In addition, correlations were examined as scatter plots to  
360 ensure that possible sensitivity not captured by the monotonic correlation coefficient was not  
361 overlooked.

## 362 2.2.2 Method to distribute 1-D simulations spatially

363 Groundwater recharge was estimated for a model domain of 82.3 km<sup>2</sup> (Fig. 1). To distribute the  
364 simulations in 1-D soil-sediment column spatially, the simulation domain was subdivided into  
365 different recharge zones, similarly to e.g. Jyrkämä et al. (2002). Zonation in the model was  
366 based on two variables: LAI and unsaturated zone thickness (UZT). The calculation of spatially  
367 distributed values for LAI and UZT is presented in detail in sections 2.1.1 and 2.1.4. Both  
368 variables were presented as a grid maps with 20m x 20m cell size with a floating point number  
369 assigned to each cell, resulting in a total of 205 708 cells for the model domain. The small  
370 model cell size was selected to ensure full exploitation of the forest inventory plots in LAI  
371 determination. The spatially distributed data were then divided into 15 classes for LAI and 30  
372 classes for UZT. The classes are primarily equal intervals, which was convenient in the

373 subsequent data processing, but in addition the frequency distributions of LAI and UZT cell  
 374 values were used to assign narrower classes for parameter ranges with many values (see  
 375 histograms in Figs. 3 and 4). Class interval for LAI was 0.2 units up to a value of 2 (class 1:  
 376 LAI = 0-0.2, etc.) and 0.3 to the maximum LAI value of 3.5. Class interval for UZT was 1 m  
 377 to 10 m depth and 2 m to the final depth of 51 m. Finally, the classified LAI and UZT data were  
 378 combined to a raster map with 20m x 20m cell size, producing 449 different zones with unique  
 379 combinations of LAI and UZT values. Spatial coupling was done with the ArcGIS software  
 380 (ESRI, 2011).

381 Variation in the LAI and UZD parameters were used to allocate the 1-D soil-sediment profile  
 382 simulations spatially to the study site. LAI class in model cell specified a subset of the 400 1-  
 383 D simulations that were applicable for a given cell. UZT class for each cell (Fig. 2) specified  
 384 the depth in the simulated 51 m soil-sediment profile where the water flux output was extracted.  
 385 Using this approach each unique recharge zone (a combination of UZT and LAI class) had on  
 386 average 27 water flow time series (number of total model runs [400] divided by number of LAI  
 387 cell classes [15]) produced by different random combinations of parameters (Table 2). Equation  
 388 (3) was used to propagate the variability in the 27 time series into the final areal recharge.

$$389 \quad R_{i,j} = \frac{\sum_{l=1}^{449} n(l) * R_{s_i,rand(1:k)} * A_c}{A_{tot}} \quad (3)$$

390 where  $R_{i,j}$  is the final sample of areal recharge [ $\text{mm day}^{-1}$ ],  $i$  is the index for simulation time  
 391 step (= 1:14975),  $j$  is the index for sample for a given time step (1:150),  $l$  is the index for unique  
 392 recharge zone,  $n(l)$  is the number of cells in a given recharge zone,  $R_s$  is the recharge sample  
 393 [ $\text{mm/day}$ ] for a given recharge zone at time step  $l$ ,  $k$  is the number of time series for a given  
 394 recharge zone,  $A_c$  is the surface area of a model raster cell ( $=20 \text{ m} * 20 \text{ m} = 400 \text{ m}^2$ ), and  $A_{tot}$   
 395 is the surface area of the total recharge area.

396 The resulting  $R$  matrix has 150 time series for areal recharge produced by simulations with  
 397 different parameter realizations. The variability between the time series provides an indication  
 398 of how much the simulated recharge varies due to different model parameter values. The  
 399 method allows computationally efficient recharge simulations, because the different recharge  
 400 zones do not all have to be simulated separately.

401 The simulation approach assumes that: (1) over the long-term, the water table remains at a  
 402 constant level, i.e. the unsaturated thickness for each model cells stays the same. Monitoring  
 403 data from 11 boreholes and seven lakes with more than 5 years of observation history shows

404 level variability of 1 – 1.5 m, with depressions and recoveries of the water table. This variability  
405 is within the accuracy of water table estimation by interpolation. (2) the capillary fringe in the  
406 sandy ~~soil-sediment~~ is thin enough not to affect the water flow before arriving at the ‘imaginary’  
407 water table at the center of each ~~soil-UZT~~ class. (3) only vertical flow takes place in the  
408 unsaturated ~~soil-sediment~~ matrix, a typical assumption in recharge estimation techniques  
409 (Dripps and Bradbury, 2010, Jyrkama et al., 2002, Scanlon et al., 2002a). (4) surface runoff is  
410 negligible primarily due to the permeable ~~soil-sediment~~ type (as noted by Keese et al., 2005),  
411 and also due to lichen cover inhibiting runoff by increasing surface roughness (Rodríguez-  
412 Caballero et al., 2012). The maximum observed daily rainfall for the area has been 57.4 mm.  
413 Further assuming that rain for the day fell only during one hour, it would equal to  $1.59 \cdot 10^{-5} \text{ m s}^{-1}$   
414 input rate of water, which is close to the lower range of saturated hydraulic conductivity at  
415 the study site ( $1.99 \cdot 10^{-5} \text{ m s}^{-1}$ ). Therefore rainstorms at the site very rarely exceed the theoretical  
416 infiltration capacity. As a field verification, surface runoff has not been observed during field  
417 visits and the area lacks intermittent or ephemeral stream networks.

### 418 2.2.3 Estimation of evapotranspiration

419 Four different evaporation processes were considered in this study (Fig. 5); soil evaporation  
420 (evaporation from the topmost soil layer, i.e. the lichen matrix), snow evaporation (evaporation  
421 from snow surface), transpiration (evaporation through the vascular system of tree canopy) and  
422 lake evaporation (evaporation from free water surface). ~~In areas with unsaturated soil zones,~~  
423 ~~the~~ first three components were estimated, along with water flow simulations, using  
424 CoupModel. However, as 3.6 % (2.9 km<sup>2</sup>) of the surface area of the study site consists of lakes  
425 (Fig. 1), lake evaporation from free water surfaces was calculated independently from the  
426 CoupModel simulations.

427 Transpiration from the Scots pine canopy ( $L_v E_{tp}$ ) was calculated using Penman-Monteith (P-  
428 M) combination (Appendix 1, Eq. 1). Whenever possible, all the parameters relating to the P-  
429 M equation were estimated based on data, namely LAI of the canopy. Surface resistance and  
430 saturation vapor pressure difference are the main factors controlling conifer forest  
431 evapotranspiration, while the aerodynamic resistance is of less importance (Lindroth, 1985,  
432 Ohta et al., 2001). In the calculation of aerodynamic resistance with the P-M equation,  
433 roughness length is related to LAI and canopy height, according to Shaw and Pereira (1982).  
434 Other parameters governing the aerodynamic resistance, except for LAI, were treated as  
435 constant. The surface resistance of the pine canopy was estimated with the Lohammar equation

436 (see e.g. Lindroth, 1985), accounting for effects of solar radiation and air moisture deficit in  
437 tree canopy gas exchange. Because LAI values have a strong influence in the surface resistance  
438 Lohammar equation, the other parameters governing the surface resistance were excluded from  
439 the Monte Carlo runs. Distribution of root biomass with respect to depth from the soil surface  
440 was presented with an exponential function, because most Scots pine roots are concentrated in  
441 the shallow soil zone. A typical root depth value of 1 m was used for the entire canopy  
442 (Kalliokoski, 2011, Kelliher et al., 1998, Vincke and Thiry, 2008). Soil and snow evaporation  
443 were calculated using an empirical approach (Appendix 1, Eq. 4) based on the P-M equation,  
444 as described in detail in Jansson and Karlberg (2004). Soil evaporation is calculated for the  
445 snow-free fraction of the soil surface, and the snow evaporation is solved separately as a part  
446 of snow pack water balance.

447 In areas where the water table is close to the ground surface, the water table can provide an  
448 additional source of water for evapotranspiration (Smerdon et al., 2008). To take into account  
449 the decreased recharge for areas with near surface water tables, the recharge for cells with an  
450 unsaturated zone of <1 m (8.3% of the study site, 6.8 km<sup>2</sup>) was estimated with a water balance  
451 approach. We assumed that for areas with a shallow water table, soil water content was not a  
452 limiting factor for transpiration. Therefore an additional water source for transpiration was  
453 considered by making the transpiration rate equal to simulated potential transpiration (T) during  
454 times when the actual transpiration was simulated (T > 0.05 mm). Increasing effect of the water  
455 table located at 1 m depth on soil evaporation was tested with simulations and found to be 5-  
456 10% higher with than without a water table. Therefore a 7% addition was made to the simulated  
457 actual soil evaporation for cells with a shallow water table. Daily recharge ( $R_{1m}$ , L T<sup>-1</sup>) for cells  
458 with unsaturated thickness below 1 m was estimated as:

$$459 R_{1m} = I - T_{adj} - ES_{adj} \quad (4)$$

460 where I is infiltration water arriving to lake/soil surface, including both meltwater from the  
461 snowpack and precipitation [L T<sup>-1</sup>],  $T_{adj}$  [mm d<sup>-1</sup>] is adjusted transpiration, and  $ES_{adj}$  [mm d<sup>-1</sup>]  
462 is adjusted soil evaporation. Kettle hole lakes in esker aquifers often lack surface water inlets  
463 and outlets and are therefore an integral part of the groundwater system (Ala-aho et al., 2013,  
464 Winter et al., 1998), so we considered these lakes as contributors to total groundwater recharge.  
465 In other words, rainfall per lake surface area is treated equally as addition to the aquifer water  
466 storage as groundwater recharge. As a difference, lake water table is subjected to evaporation  
467 unlike the groundwater table. Lake evaporation ( $E_{lake}$ ) was estimated with the mass transfer

468 approach (see e.g. Dingman, 2008) according to Eq. (7) in Appendix 1. The mass transfer  
469 method was selected because of its simplicity, daily output resolution, low data requirement,  
470 and physically-based approach. However various calculation methods could easily be used in  
471 the modelling framework, depending on the data availability (see e.g. Rosenberry et al., 2007).  
472 If lake percentage in the area of interest is high, more sophisticated methods may be required  
473 to better represent the system. For the Rokua site the bias introduced by a simplistic approach  
474 was considered minor.

### 475 **2.3 Model validation**

476 Model performance was tested by comparing the simulated recharge values with two  
477 independent recharge estimates in local and regional scale; the water table fluctuation (WTF)  
478 method and base flow estimation, respectively. The WTF method is routinely used to estimate  
479 groundwater recharge because of its simplicity and ease of use. It assumes that any rise in water  
480 level in an unconfined aquifer is caused by recharge arriving at the water table. For a detailed  
481 description of the method and its limitations, see e.g. Healy and Cook (2002). The recharge  
482 amount ( $R$ ,  $L T^{-1}$ ) is calculated based on the water level prior to and after the recharge event  
483 and the specific yield of the ~~soil~~sandy sediments:

$$484 R = S_y \frac{\Delta h}{\Delta t} \quad (5)$$

485 where  $S_y$  is the specific yield,  $h$  is the water table height [L], and  $t$  is the time of water table rise  
486 [T].

487 The WTF method requires groundwater level data with adequate resolution for both time and  
488 water level, to identify periods of rising and falling water table. Water table was monitored  
489 using pressure-based dataloggers (Solinst Levellogger Gold) recording with hourly interval  
490 from six water table wells with average unsaturated zone thicknesses of 1.2, 1.6, 5.0, 8.0, 9.3,  
491 and 14.7 m (Fig. 1). Wells where the water table was <2 m from the ground surface responded  
492 to major precipitation events. In the deeper wells, only the recharge from snowmelt was seen  
493 as water table rise. Estimates of the ~~soil~~sandy sediment specific yield are required for the  
494 calculations (Eq. 5), but no ~~soil~~sediment samples were available from the wells used in water  
495 table monitoring. Drilling records for these wells reported fine and medium sand, which was  
496 consistent with the particle size distribution for other wells in the area. Therefore an estimated  
497 value of 0.20-0.25 for the specific yield of all wells was used, according to typical values for  
498 fine and medium sand (Johnson, 1967).



499 The recharge estimated with the WTF method was compared with the simulated recharge  
500 during the recorded water level rise in the well. For each well, the cumulative sum of simulated  
501 water flow was extracted from soil-sediment profile depth corresponding to well water table  
502 depth. As an example, the simulated recharge in well ROK1 (unsaturated thickness on average  
503 14.7 m) was extracted from soil-UTZ class 12, corresponding to recharge for unsaturated  
504 thickness of 14-16 m. All 400 model runs were used, providing 400 estimates for recharge for  
505 each time period of recorded water level rise.

506 A regional estimate of groundwater recharge was estimated as baseflow of streams originating  
507 at the groundwater discharge area. Because the Rokua esker aquifer acts as a regional water  
508 divide, stream flow was monitored around the esker, in total of 18 locations (Fig. 1). The flows  
509 were measured total of 8 times between 6 July 2009 and 3 August 2010 (see Rossi et al., 2014).  
510 The lowest total outflow during 9-10 February 2010 was recorded after three months of snow  
511 cover period, when water contribution to streams from surface runoff was minimal. The  
512 minimum outflow was considered as baseflow from the aquifer reflecting long term  
513 groundwater recharge in the area.

514

## 515 **3 Results**

### 516 **3.1 Model validation with the WTF and baseflow methods**

517 Model validation showed that the modeling approach could reasonably reproduce (1) the main  
518 groundwater recharge events when compared to the WTF method (Fig. 6) and (2) the regional  
519 level of recharge compared to stream baseflow. The WTF method agreed well with the  
520 simulated values, with overlapping estimates between the methods for all but two recharge  
521 events. Also the median value of simulations was close to WTF method, with some bias to  
522 higher estimates from the simulations. The discrepancy can be due to very different assumptions  
523 behind the methods and uncertainty in local parameterization; in the WTF method for the  
524 specific yield ( $S_y$ ) and for simulations mainly the hydraulic conductivity which dictates the  
525 simulated timing of recharge. Uncertainty in the  $S_y$  estimate is acknowledged by showing  $S_y$  a  
526 range rather than a single value (Fig. 6), but still  $S_y$  is not truly known for the location of  
527 observation boreholes. Simplifying assumptions and subjective interpretation of both timing  
528 and height of water table rise create additional inaccuracies in the WTF estimate.

529 Independent regional estimate of recharge, stream baseflow, was 70 500 m<sup>3</sup> s<sup>-1</sup>, or 312.7 mm  
530 a<sup>-1</sup> when related to the recharge area. The order of magnitude agreed with long term simulated  
531 average of 362.8 mm a<sup>-1</sup>. Typical error in individual stream flow measurements is within 3-6 %  
532 of the measured value (Sauer and Meyer, 1992), which brings minor uncertainty in the baseflow  
533 value. The smaller value for stream baseflow compared to simulated long term average recharge  
534 can be explained with conceptual understanding of site hydrogeology (Ala-aho et al., 2015,  
535 Ala-aho et al., 2013, Rossi et al., 2012, Rossi et al., 2014). Part of the recharged groundwater  
536 does not discharge to the small streams whose baseflow was measured, but flows underneath  
537 the stream catchments and seeps out to regional surface bodies (Lake Oulujärvi and River  
538 Oulujoki) further away from the recharge area (Fig. 2). Fully integrated surface-subsurface  
539 hydrological modeling study of the same site presented in Ala-aho et al. (2015) simulated an  
540 outflow of 79 mm a<sup>-1</sup> to regional surface water bodies.

### 541 **3.2 Temporal variations in groundwater recharge**

542 When recharge simulation time series were summarized to annual values (1 Oct-30 Sept),  
543 recharge rates co-varied with annual infiltration with linear correlation coefficient of 0.89  
544 (Fig. 7) as expected based on previous work in humid climate and sandy ~~soils~~ aquifers (Keese  
545 et al., 2005, Lemmelä, 1990). Both annual recharge and infiltration displayed an increasing  
546 trend. The plot also showed the level of uncertainty in annual recharge values introduced by  
547 differences in model parameterization (black area). The difference between minimum and  
548 maximum value for simulated annual recharge was on average 23.0 mm. Thus the variability in  
549 recharge estimates was 6.3 % of mean annual recharge 362.8 mm.

550 According to the simulations, the *effective rainfall*, i.e. the percentage of corrected rainfall  
551 resulting in groundwater recharge annually, was on average 59.3%. This is in agreement with  
552 previous studies on unconfined esker aquifers at northerly latitudes, in which the proportion of  
553 annual precipitation percolating to recharge is reported to be 50-70% (71% by Zaitsoff (1984),  
554 54% by Lemmelä and Tattari (1986) and 56% by Lemmelä (1990)). The percentage of effective  
555 rainfall varied considerably, by almost 30 %-units, between different hydrological years, from  
556 44.8% in some years up to 73.1% in others.

### 557 3.3 Influence of LAI on spatial variation of groundwater recharge

558 The spatial distribution of groundwater recharge was mostly due to variations in LAI, but also  
559 influenced by distance to water table, and distribution of lakes (Fig. 8). Higher evaporation rates  
560 from lakes led to lower recharge in lakes (see red spots in Fig. 8). Similarly, high LAI led to  
561 high ET and resulted in low recharge in plots with high LAI. Other areas of low recharge,  
562 although not as obvious at the larger spatial scales shown in Fig. 8, were cells with a shallow  
563 water table (section 2.2.2). The effect of high ET at locations with a shallow water table can  
564 best be seen in south-east parts of the aquifer.

565 Kendall correlation analysis of simulation parameters and annual average model outputs  
566 identified LAI as the most important parameter controlling evapotranspiration and infiltration  
567 (Table 3). Parameters related to ~~soil-sediment~~ hydraulics and evaporation showed some  
568 sensitivity to simulation results, while the parameters for lichen vegetation were only slightly  
569 sensitive or insensitive to simulation output variables. The LAI parameter governed the level  
570 of evaporation for different ET components (Fig. 9). Evaporation from soil (and snow)  
571 compensated for mean annual ET for LAI values up to around 1.0, after which total ET  
572 increased as a function of LAI.

573 The scenarios for low (0 ... 0.2) and high (3.2 ... 3.5) LAI changed the groundwater recharge  
574 rates compared to the current LAI distribution (in Fig. 7). In the high LAI scenario the annual  
575 recharge was on average 101.7 mm lower than in the low LAI scenario. These results suggest  
576 that management of the Scots pine canopy has a significant control on the total recharge rates  
577 in unconfined esker aquifers.

578 Average land surface ET components remained relatively constant between years, but the  
579 simulated ET displayed a wide spread between simulations (Fig. 10). Estimated annual  
580 evapotranspiration (mean 237.6 mm) was somewhat lower than previous regional estimates of  
581 total ET (300 mm; (Mustonen, 1986)). Lake evaporation rates were generally higher than  
582 evapotranspiration from the land surface (420.0 mm). The variation in simulated lake  
583 evaporation was considerably lower than that in ET, as a different approach was used to account  
584 for uncertainty in the simulations. Transpiration showed greater variation between simulations  
585 than soil evaporation and total land surface ET. On average, transpiration also comprised a  
586 slightly larger share of total evaporation than soil evaporation. Simulated snow evaporation was  
587 a small, yet not insignificant, component in the total ET.

#### 588 4 Discussion

589 The method used here to estimate LAI from forestry inventories introduces a new approach for  
590 incorporating large spatial coverage of detailed conifer canopy data into groundwater recharge  
591 estimations. LAI values reported for conifer forests in Nordic conditions similar to the study  
592 site are in the range 1-3, depending on canopy density and other attributes (Koivusalo et al.,  
593 2008, Rautiainen et al., 2012, Vincke and Thiry, 2008, Wang et al., 2004). The LAI values  
594 obtained for the study site (mean 1.25) were at the lower end of this range. Furthermore, the  
595 data showed a bimodal distribution, with many model cells with low LAI ( $< 0.4$ ) lowering the  
596 mean LAI. The low LAI values were expected because of active logging and clearcutting  
597 activities in the study area. Although the equations to estimate LAI are empirical in nature and  
598 based on simplified assumptions, the method can outline spatial differences in canopy structure.  
599 Wider use of this method in Finland is practically possible, as active forestry operations in  
600 Finland have yielded an extensive database on canopy coverage, which could be used in  
601 groundwater management. However, the LAI estimation method could be further validated with  
602 field measurements or Lidar techniques (Chasmer et al., 2012, Riaño et al., 2004).

603 Plant cover, represented as LAI, proved to be the most important model parameter important  
604 parameter controlling total ET, and thereby the amount of groundwater recharge (Table 3, Fig.  
605 9). The LAI parameter was included in the equations controlling both transpiration and soil  
606 evaporation, and therefore the sensitivity of the parameter is not surprising. While soil  
607 evaporation partly compensated for the lower transpiration with low LAI values, the total  
608 annual ET values progressively increased as a function of LAI (Fig. 9). Interestingly, the  
609 simulations suggested that ET remains constant at constant level in the LAI range 0-1,  
610 potentially due to the sparse canopy changing the aerodynamic resistance and partitioning of  
611 radiation limiting soil evaporation, while still not contributing much to transpiration in total ET.  
612 This implies that the maximum groundwater recharge for boreal Scots pine remains rather  
613 constant up to a threshold LAI value of around 1. This knowledge can be used when co-  
614 managing forest and groundwater resources in order to optimize both.

615 Importance of LAI has been reported in earlier studies estimating groundwater recharge  
616 (Dripps, 2012, Keese et al., 2005, Sophocleous, 2000), but here the vegetation was represented  
617 with more spatially detailed patterns and a field data-based approach for LAI. According to  
618 previous studies, average ET from boreal conifer forests is around  $2 \text{ mm d}^{-1}$  during the growing  
619 season (Kelliher et al., 1998), which is similar to our average value of  $1.6 \text{ mm d}^{-1}$  for the period

620 1 May-31 Oct. Some earlier studies have claimed that the influence of LAI on total ET rates  
621 from boreal conifer canopies is minor (Kelliher et al., 1993, Ohta et al., 2001, Vesala et al.,  
622 2005), but our simulation results indicate that higher LAI values lead to higher total ET values.  
623 The simulations showed that variable intensity of forestry, from low canopy coverage (LAI =  
624 0-0.2) to dense coverage (LAI = 3.2-3.5) resulted in a difference of over 100 mm in annual  
625 recharge (Fig. 7). It can be argued that the scenarios are unrealistic, because high LAI values,  
626 covering the whole study site, may not be achieved even with a complete absence of forestry  
627 operations. Nevertheless, the result demonstrates a substantial impact of forestry operations on  
628 esker aquifer groundwater resources. The lichen layer covering the soil surface was explicitly  
629 accounted for in the simulation set-up, which to our knowledge is a novel modification. Kelliher  
630 et al. (1998) concluded that precipitation intercepted by lichen was an important source of  
631 understorey evaporation, especially directly after rain events. In addition, Bello and Arama  
632 (1989) reported that lichen could intercept light rain showers completely and that only intense  
633 rain events caused drainage from lichen canopy to mineral soil. While the lichen layer might  
634 have an increasing effect on soil evaporation through ‘interception storage’, Fitzjarrald and  
635 Moore (1992) suggest that a lichen cover may in fact have an insulating influence on heat and  
636 vapor exchange between soil and atmosphere, therefore impeding evaporation from the mineral  
637 soil. In the present study, the lichen layer appeared to have minor influence on total evaporation,  
638 soil evaporation and infiltration, as these variables showed only little sensitivity to lichen B&C  
639 parameters (Table 3). However, the approach to represent lichen with B&C model needs to  
640 better examined, as water retention capacity of lichen layer was ~~treated-introduced to the~~  
641 ~~simulations equal-using the concept of total-~~porosity, which is not strictly coherent with the  
642 ~~Brooks and Corey (B&C)~~ model. Nevertheless, the used approach successfully produced an  
643 additional ~~dynamic~~ interception storage of water in the correct range (generally 3-7 mm  
644 depending on random parameterization, data not shown). The performed laboratory  
645 measurement of lichen water retention should be supplemented with detailed analysis of lichen  
646 pressure-saturation curve and hydraulic conductivity to clarify the role of lichen in soil  
647 evaporation, and thereby groundwater recharge.

648 Stochastic variation of selected model parameters illustrated the uncertainties relating to  
649 numerical recharge estimation using the Richards equation in one dimension. The capability  
650 and robustness of the Richards equation to reproduce soil water content and water fluxes have  
651 been demonstrated extensively in various studies (Assefa and Woodbury, 2013, Scanlon et al.,  
652 2002b, Stähli et al., 1999, Wierenga et al., 1991). Therefore we considered that model

Commented [PA2]: Point #1; discussion slightly modified

653 calibration and validation with point observations of variables such as soil volumetric water  
654 content or soil temperature would not provide novel insights into water flow in unsaturated  
655 ~~soil~~porous media. Instead, we incorporated the parameter uncertainty ranges, usually used in  
656 model calibration, to the final recharge simulation output. An important outcome was that the  
657 uncertainty in the model output caused by different model parameterizations was small in  
658 comparison with the interannual variation in recharge. The error caused by uncertainty in the  
659 model assumptions or driving climate data was not addressed in this study.

660 The sensitivity analysis focused on total cumulative values of fluxes and did not address the  
661 temporal variations in the variables. Soil-Sediment hydraulic parameters mainly influenced the  
662 timing of recharge through residence time in the ~~soil~~unsaturated zone, not so much the total  
663 amount. Therefore the ~~soil-sediment~~ hydraulic parameters showed only minor sensitivity,  
664 perhaps misleadingly. It should be noted that vertical heterogeneity in the ~~soil-unsaturated~~  
665 sediment profile hydraulic parameters can reduce the total recharge rates (Keese et al., 2005).  
666 However, vertical heterogeneities were ignored in this study not only to simplify the model, but  
667 also because the drilling logs showed only little variation in the area. Work of Wierenga et al.  
668 (1991) supports the simplification by showing that excluding moderate vertical heterogeneities  
669 does not significantly affect the performance of water flow simulations with the Richards  
670 equation.

671 Simulations acknowledged shallow water table contribution to evapotranspiration in an  
672 indirect, conceptual approach. Including a water table fixed at different depths in the ~~soil~~  
673 sediment profile would have been possible in the CoupModel setup. Influence of water table  
674 fixed at 2 m depth was tested and found to increase ET 3.5% for LAI values of 3, but for LAI  
675 values of 0.5 and 1.5 the increase in ET was only trivial. We expect only minor increase in ET  
676 with deeper water table configuration (with the given ~~soil-type~~sediment texture), and therefore  
677 argue that excluding water table results in only minimal overestimation of total recharge at the  
678 study site. It should be noted that upward water fluxes were not excluded from the water flow  
679 time series and negative fluxes were considered as “negative recharge” at any depth. The  
680 simplification is made that water available for upward fluxes comes only from the soil moisture  
681 storage, not from the water table.

682 According to the simulations, the percentage of precipitation forming groundwater recharge  
683 varied considerably between years, as also reported in previous studies on transient recharge  
684 (Assefa and Woodbury, 2013, Dripps and Bradbury, 2010). Even though annual recharge was

685 correlated with annual precipitation, and therefore years with high precipitation resulted in  
686 higher absolute recharge (Fig. 7), the percentage of effective rainfall did not increase as a  
687 function of annual sum of precipitation. This is somewhat surprising, because the rather  
688 constant evaporation potential between years (Fig. 10) and high soil-sediment hydraulic  
689 conductivity could be expected to result in a higher percentage of rainfall reaching the water  
690 table in rainy years. Some studies (Dripps and Bradbury, 2010, Okkonen and Kløve, 2010) have  
691 suggested that when the main annual water input arrives as snowmelt during the low  
692 evaporation season, it is likely to result in higher percentage recharge than in a year with little  
693 snow storage and precipitation distributed evenly throughout summer and autumn, which may  
694 contribute to the variability in the effective rainfall coefficient. However, when the maximum  
695 annual SWE value was used as a proxy for annual snow storage, there was no evidence of snow  
696 amount explaining the interannual variability in the recharge coefficient. Other factors  
697 contributing to recharge coefficient variability may be related to soil moisture conditions prior  
698 to snowfall, or the intensity of summer precipitation events (Smerdon et al., 2008, Stähli et al.,  
699 1999).

700 The above-mentioned reasons make the concept of effective rainfall, which is currently  
701 routinely used to estimate groundwater recharge for groundwater management in e.g. Finland  
702 (Britschgi et al., 2009), susceptible to over- or under-estimation of actual annual recharge. This  
703 applies especially for aquifers with a thick unsaturated zone, where rainy years produce higher  
704 average recharge with some delay and for a longer duration (Zhou, 2009).

705

## 706 **5 Conclusions**

707 A physically-based approach to simulate groundwater recharge for sandy unconfined aquifers  
708 in cold climates was developed. The method accounts for the influence of vegetation,  
709 unsaturated zone thickness, presence of lakes, and uncertainty in simulation parameters in the  
710 recharge estimate. It is capable of producing spatially and temporally distributed groundwater  
711 recharge values with uncertainty margins, which are generally lacking in recharge estimates,  
712 despite understanding of uncertainty related to recharge estimates being potentially crucial for  
713 groundwater resource management. However, the parameter uncertainty defined for the study  
714 area was of minor significance compared with interannual variations in the recharge rates  
715 introduced by climate variations.

716 The simulations showed that Scots pine canopy, parameterized as leaf area index (LAI), was  
717 important in controlling the total amount of groundwater recharge. Forestry inventory databases  
718 were used to estimate and spatially allocate the LAI and the results showed that such inventories  
719 could be better utilized in groundwater resource management. Forest cuttings were  
720 demonstrated to increase groundwater recharge significantly. A sensitivity analysis on the  
721 parameters used showed that soil evaporation could compensate for low LAI-related  
722 transpiration up to a LAI value of approximately 1, which may be important in finding the  
723 optimal level for forest management in groundwater resource areas. The concept of effective  
724 rainfall gave inconsistent estimates of recharge in annual timescales, showing the importance  
725 of using physically-based recharge estimation methods for sustainable groundwater recharge  
726 management.

727

728

729

730

#### 731 **Author contribution**

732 P. Ala-aho and P.M Rossi collected and analyzed the field data. P. Ala-aho designed the  
733 simulation set-up, performed the simulations and interpreted the results. P. Ala-aho prepared  
734 the manuscript with contributions from all co-authors.

735

#### 736 **Acknowledgements**

737 This study was made possible by the funding from EU 7th Framework programme GENESIS  
738 (Contract Number 226536), Academy of Finland AKVA research program, the Renlund  
739 Foundation, VALUE doctoral school and Maa- ja vesitekniiikantuki ry. We would like to  
740 express our gratitude to Geological survey of Finland, Finnish Forest Administration  
741 (Metsähallitus) and Finnish Forest Centre (Metsäkeskus), Finnish meteorological institute,  
742 Finnish environmental administration and National land survey of Finland for providing  
743 datasets and expert knowledge that made this study possible in its current extent. To reproduce  
744 the research in the paper, data from above mentioned agencies can be made available for  
745 purchase on request from the corresponding agency, other data can be provided by the



746 corresponding author upon request. We thank Per-Erik Jansson for his assistance with the  
747 CoupModel and Jarkko Okkonen (GTK), ~~and two~~ anonymous reviewer, and Angelo Basiles for  
748 their critical comments that significantly improved the manuscript.

749

750

751

752

753

754

755

756

757

758

759

760

761

762

763

764

765

766

767

768

769

770

771

772 **References**

- 773 Aartolahti, T.: Morphology, vegetation and development of Rokuanvaara, an esker and dune  
774 complex in Finland, *Societas geographica Fenniae*, Helsinki, 1973.
- 775 Ala-aho, P., Rossi, P. M. and Kløve, B.: Interaction of esker groundwater with headwater  
776 lakes and streams, *J. Hydrol.*, 500, 144-156, doi:10.1016/j.jhydrol.2013.07.014, 2013.
- 777 Ala-aho, P., Rossi, P. M., Isokangas, E. and Kløve, B.: Fully integrated surface–subsurface  
778 flow modelling of groundwater–lake interaction in an esker aquifer: Model verification with  
779 stable isotopes and airborne thermal imaging, *J. Hydrol.*, 522, 391-406,  
780 doi:10.1016/j.jhydrol.2014.12.054, 2015.
- 781 Allen, R., Pereira, L., Raes, D. and Smith, M.: Crop evapotranspiration - Guidelines for  
782 computing crop water requirements, Food and Agriculture Organization of the United  
783 Nations, Rome, 1998.
- 784 Assefa, K. A. and Woodbury, A. D.: Transient, spatially- varied groundwater recharge  
785 modelling, *Water Resour. Res.*, 49, 1-14, doi:10.1002/wrcr.20332, 2013.
- 786 Banerjee, I., McDonald, B.C.: Nature of esker sedimentation, in: *Glaciofluvial and*  
787 *Glaciolacustrine Sedimentation*, edited by: Jopling, A. V. and McDonald, B. C., *Soc. Econ.*  
788 *Paleontol. Mineral.*, Tulsa, U.S.A, 132-155, 1975
- 789 Bello, R. and Arama, A.: Rainfall interception in lichen canopies, *Climatol. Bull.*, 23, 74-78,  
790 1989.
- 791 Bent, G. C.: Effects of forest-management activities on runoff components and ground-water  
792 recharge to Quabbin Reservoir, central Massachusetts, *For. Ecol. Manage.*, 143, 115-129,  
793 2001.
- 794 Blum, O. B.: Water relations, in: *The lichens*, Ahmadjian, V. and Hale, M. E. (Eds.),  
795 Academic Press Inc., USA, 381-397, 1973.
- 796 Bolduc, A., Paradis, S. J., Riverin, M., Lefebvre, R. and Michaud, Y.: A 3D esker geomodel  
797 for groundwater research: the case of the Saint-Mathieu–Berry esker, Abitibi, Quebec,  
798 Canada, in: *Three-Dimensional Geologic Mapping for Groundwater Applications: workshop*  
799 *extended abstracts*, 17-20, Salt Lake City, Utah, 15 Oct, 2005.
- 800 Britschgi, R., Antikainen, M., Ekholm-Peltonen, M., Hyvärinen, V., Nylander, E., Siiro, P.  
801 and Suomela, T.: Mapping and classification of groundwater areas, *The Finnish Environment*  
802 *Institute*, Sastamala, Finland, 75 pp., 2009.
- 803 Chasmer, L., Pertrone, R., Brown, S., Hopkinson, C., Mendoza, C., Diiwu, J., Quinton, W.  
804 and Devito, K.: Sensitivity of modelled evapotranspiration to canopy characteristics within  
805 the Western Boreal Plain, Alberta, in: *Remote Sensing and Hydrology*, Proceedings of a  
806 Symposium at Jackson Hole, 337-341, Wyoming, USA, 27-30 September 2010, 2012.

807 Croteau, A., Nastev, M. and Lefebvre, R.: Groundwater recharge assessment in the  
808 Chateauguay River watershed, *Canadian Water Resources Journal*, 35, 451-468, 2010.

809 Dingman, S. L.: *Physical hydrology*, Waveland Press Inc, Long Grove, IL, 2008.

810 Dripps, W.: An Integrated Field Assessment of Groundwater Recharge, *Open Hydrology*  
811 *Journal*, 6, 15-22, 2012.

812 Dripps, W. and Bradbury, K.: The spatial and temporal variability of groundwater recharge in  
813 a forested basin in northern Wisconsin, *Hydrol. Process.*, 24, 383-392, doi:10.1002/hyp.7497,  
814 2010.

815 Dripps, W. and Bradbury, K.: A simple daily soil–water balance model for estimating the  
816 spatial and temporal distribution of groundwater recharge in temperate humid areas,  
817 *Hydrogeol. J.*, 15, 433-444, doi:10.1007/s10040-007-0160-6, 2007.

818 EC: Directive 2006/118/EC of the European Parliament and of the Council on the protection  
819 of groundwater against pollution and deterioration, Brussels, Belgium, 2006.

820 ESRI: ArcGIS Desktop: Release 10, Environmental Systems research institute, Redlands,  
821 Texas, 2011.

822 Finnish environmental administration: Oiva – the environmental and geographical  
823 information service, Helsinki, Finland, Observation station number 5903320, Data extracted  
824 27 June 2013, 2013.

825 Finnish environmental administration: Oiva – the environmental and geographical  
826 information service, Helsinki, Finland, Observation station number 1592101, Data extracted  
827 11 Feb 2011, 2011.

828 Fitzjarrald, D. R. and Moore, K. E.: Turbulent transports over tundra, *J. Geophys. Res.*, 97,  
829 16717-16729, 1992.

830 Healy, R. W. and Cook, P. G.: Using groundwater levels to estimate recharge, *Hydrogeol. J.*,  
831 10, 91-109, 2002.

832 Hunt, R. J., Prudic, D. E., Walker, J. F. and Anderson, M. P.: Importance of unsaturated zone  
833 flow for simulating recharge in a humid climate, *Ground Water*, 46, 551-560, 2008.

834 Jansson, P. and Karlberg, L.: Coupled heat and mass transfer model for soil-plant-atmosphere  
835 systems, Royal Institute of Technology, Dept of Civil and Environmental Engineering,  
836 Stockholm, 435 pp., 2004.

837 Johnson, A. I.: *Specific yield: compilation of specific yields for various materials*, US  
838 Government Printing Office, Washington, 1967.

839 Jyrkama, M. I. and Sykes, J. F.: The impact of climate change on spatially varying  
840 groundwater recharge in the grand river watershed (Ontario), *J. Hydrol.*, 338, 237-250, 2007.

841 Jyrkama, M. I., Sykes, J. F. and Normani, S. D.: Recharge estimation for transient ground  
842 water modeling, *Ground Water*, 40, 638-648, 2002.

843 Kalliokoski, T.: Root system traits of Norway spruce, Scots pine, and silver birch in mixed  
844 boreal forests: an analysis of root architecture, morphology, and anatomy, Ph.D. thesis,  
845 Department of Forest Sciences, Faculty of Agriculture and Forestry, University of Helsinki,  
846 2011.

847 Karjalainen, T., Rossi, P., Ala-aho, P., Eskelinen, R., Reinikainen, K., Kløve, B., Pulido-  
848 Velazquez, M. and Yang, H.: A decision analysis framework for stakeholder involvement and  
849 learning in groundwater management, *Hydrol. Earth Syst. Sci.* 17, 5141-5153,  
850 doi:10.5194/hess-17-1-2013, 2013.

851 Keese, K. E., Scanlon, B. R. and Reedy, R. C.: Assessing controls on diffuse groundwater  
852 recharge using unsaturated flow modeling, *Water Resour. Res.*, 41, W06010,  
853 doi:10.1029/2004WR003841, 2005.

854 Kelliher, F. M., Leuning, R. and Schulze, E. D.: Evaporation and canopy characteristics of  
855 coniferous forests and grasslands, *Oecologia*, 95, 153-163, 1993.

856 Kelliher, F. M., Lloyd, J., Arneeth, A., Byers, J. N., McSeveny, T. M., Milukova, I., Grigoriev,  
857 S., Panfyorov, M., Sogatchev, A., Varlargin, A., Ziegler, W., Bauer, G. and Schulze, E. -:  
858 Evaporation from a central Siberian pine forest, *J. Hydrol.*, 205, 279-296,  
859 doi:10.1016/S0022-1694(98)00082-1, 1998.

860 Kløve, B., Ala-aho, P., Bertrand, G., Boukalova, Z., Ertürk, A., Goldscheider, N., Ilmonen, J.,  
861 Karakaya, N., Kupfersberger, H., Kværner, J., Lundberg, A., Mileusnić, M., Moszczynska,  
862 A., Muotka, T., Preda, E., Rossi, P., Siergieiev, D., Šimek, J., Wachniew, P., Angheluta, V.  
863 and Widerlund, A.: Groundwater dependent ecosystems. Part I: Hydroecological status and  
864 trends, *Environ. Sci. & Policy*, 14, 770-781, doi:10.1016/j.envsci.2011.04.002, 2011.

865 Koivusalo, H., Ahti, E., Laurén, A., Kokkonen, T., Karvonen, T., Nevalainen, R. and Finér,  
866 L.: Impacts of ditch cleaning on hydrological processes in a drained peatland forest,  
867 *Hydrol. Earth Syst. Sci.*, 12, 1211-1227, 2008.

868 Koundouri, P., Kougea, E., Stithou, M., Ala-Aho, P., Eskelinen, R., Karjalainen, T. P., Klove,  
869 B., Pulido-Velazquez, M., Reinikainen, K. and Rossi, P. M.: The value of scientific  
870 information on climate change: a choice experiment on Rokua esker, Finland, *Journal of*  
871 *Environmental Economics and Policy*, 1, 85-102, 2012.

872 Kumpula, J., Colpaert, A. and Nieminen, M.: Condition, potential recovery rate, and  
873 productivity of lichen (*Cladonia* spp.) ranges in the Finnish reindeer management area, *Arctic*,  
874 53, 152-160, 2000.

875 Kurki, V., Lipponen, A. and Katko, T.: Managed aquifer recharge in community water  
876 supply: the Finnish experience and some international comparisons, *Water Int.*, 38, 774-789,  
877 2013.

878 Lagergren, F., Lankreijer, H., Kučera, J., Cienciala, E., Mölder, M. and Lindroth, A.:  
879 Thinning effects on pine-spruce forest transpiration in central Sweden, *For. Ecol. Manage.*,  
880 255, 2312-2323, 2008.

881 Larson, D. W.: Lichen water relations under drying conditions, *New Phytol.*, 82, 713-731,  
882 doi:10.1111/j.1469-8137.1979.tb01666.x, 1979.

883 Lemmelä, R. and Tattari, S.: Infiltration and variation of soil moisture in a sandy aquifer,  
884 *Geophysica*, 22, 59-70, 1986.

885 Lemmelä, R.: Water balance of sandy aquifer at Hyrylä in southern Finland, Ph.D. thesis,  
886 University of Turku, Turku, 1990.

887 Lindroth, A.: Canopy Conductance of Coniferous Forests Related to Climate, *Water Resour.*  
888 *Res.*, 21, 297-304, doi:10.1029/WR021i003p00297, 1985.

889 Mustonen, S.: *Sovellettu hydrologia, Vesiyhdistys*, Helsinki, 1986.

890 National Land Survey of Finland: NLS file service of open data, Laser scanning point cloud  
891 (LiDAR), 2012.

892 Odong, J.: Evaluation of empirical formulae for determination of hydraulic conductivity  
893 based on grain-size analysis, *Journal of American Science*, 3, 54-60, 2007.

894 Ohta, T., Hiyama, T., Tanaka, H., Kuwada, T., Maximov, T. C., Ohata, T. and Fukushima, Y.:  
895 Seasonal variation in the energy and water exchanges above and below a larch forest in  
896 eastern Siberia, *Hydrol. Process.*, 15, 1459-1476, doi:10.1002/hyp.219, 2001.

897 Okkonen, J.: Groundwater and its response to climate variability and change in cold snow  
898 dominated regions in Finland: methods and estimations, Ph.D. thesis, University of Oulu,  
899 Oulu, Finland, 78 pp., 2011.

900 Okkonen, J. and Kløve, B.: A conceptual and statistical approach for the analysis of climate  
901 impact on ground water table fluctuation patterns in cold conditions, *J. Hydrol.*, 388, 1-12,  
902 doi:10.1016/j.jhydrol.2010.02.015, 2010.

903 Okkonen, J. and Kløve, B.: A sequential modelling approach to assess groundwater–surface  
904 water resources in a snow dominated region of Finland, *Journal of Hydrology*, 411, 91-107,  
905 doi:10.1016/j.jhydrol.2011.09.038, 2011.

906 Rautiainen, M., Heiskanen, J. and Korhonen, L.: Seasonal changes in canopy leaf area index  
907 and moDis vegetation products for a boreal forest site in central Finland, *Boreal*  
908 *Environ. Res.*, 17, 72-84, 2012.

909 Repola, J., Ojansuu, R. and Kukkola, M.: Biomass functions for Scots pine, Norway spruce  
910 and birch in Finland, Finnish Forest Research Institute (METLA), Helsinki, 28 pp., 2007.

911 Riaño, D., Valladares, F., Condés, S. and Chuvieco, E.: Estimation of leaf area index and  
912 covered ground from airborne laser scanner (Lidar) in two contrasting forests, *Agric. For.*  
913 *Meteorol.*, 124, 269-275, 2004.

914 Rodríguez-Caballero, E., Cantón, Y., Chamizo, S., Afana, A. and Solé-Benet, A.: Effects of  
915 biological soil crusts on surface roughness and implications for runoff and erosion,  
916 *Geomorphology*, 145, 81-89, 2012.

917 Rosenberry, D. O., Winter, T. C., Buso, D. C. and Likens, G. E.: Comparison of 15  
918 evaporation methods applied to a small mountain lake in the northeastern USA, *Journal of*  
919 *Hydrology*, 340, 149-166, 2007.

920 Rossi, P. M., Ala-aho, P., Ronkanen, A. and Kløve, B.: Groundwater - surface water  
921 interaction between an esker aquifer and a drained fen, *J. Hydrol.*, 432-433, 52-60,  
922 doi:10.1016/j.jhydrol.2012.02.026, 2012.

923 Rossi, P. M., Ala-aho, P., Doherty, J. and Kløve, B.: Impact of peatland drainage and  
924 restoration on esker groundwater resources: modeling future scenarios for management,  
925 *Hydrogeol. J.*, doi:10.1007/s10040-014-1127-z, 2014.

926 Rothacher, J.: Increases in water yield following clear-cut logging in the Pacific Northwest,  
927 *Water Resour. Res.*, 6, 653-658, 1970.

928 Sauer, V. B. and Meyer, R.W.: Determination of error in individual discharge measurements.  
929 Open-File Report 92-144. U.S. Geological Survey, Norcross, Georgia, 1992.

930 Scanlon, B. R., Healy, R. and Cook, P.: Choosing appropriate techniques for quantifying  
931 groundwater recharge, *Hydrogeol. J.*, 10, 91-109, 2002.

932 Scanlon, B. R., Christman, M., Reedy, R. C., Porro, I., Simunek, J. and Flerchinger, G. N.:  
933 Intercode comparisons for simulating water balance of surficial sediments in semiarid regions,  
934 *Water Resour. Res.*, 38, 59-1-59-16, doi:10.1029/2001WR001233, 2002.

935 Scibek, J. and Allen, D.: Modeled impacts of predicted climate change on recharge and  
936 groundwater levels, *Water Resour. Res.*, 42, W11405, doi:10.1029/2005WR004742, 2006.

937 Shaw, R. H. and Pereira, A. R.: Aerodynamic roughness of a plant canopy: A numerical  
938 experiment, *Agricultural Meteorology*, 26, 51-65, doi:10.1016/0002-1571(82)90057-7, 1982.

939 Smerdon, B., Mendoza, C. and Devito, K.: Influence of subhumid climate and water table  
940 depth on groundwater recharge in shallow outwash aquifers, *Water Resour. Res.*, 44,  
941 W08427, doi:10.1029/2007WR005950, 2008.

942 Sophocleous, M.: Quantification and regionalization of ground-water recharge in south-  
943 central Kansas: integrating field characterization, statistical analysis, and GIS, *Spec Issue,*  
944 *Compass*, 75, 101-115, 2000.

945 Stähli, M., Jansson, P. and Lundin, L. C.: Soil moisture redistribution and infiltration in  
946 frozen sandy soils, *Water Resour. Res.*, 35, 95-103, 1999.

947 Vesala, T., Suni, T., Rannik, Ü, Keronen, P., Markkanen, T., Sevanto, S., Grönholm, T.,  
948 Smolander, S., Kulmala, M. and Ilvesniemi, H.: Effect of thinning on surface fluxes in a  
949 boreal forest, *Global Biogeochem. Cycles*, 19, GB2001, doi:10.1029/2004GB002316, 2005.

950 Vincke, C. and Thiry, Y.: Water table is a relevant source for water uptake by a Scots pine  
951 (*Pinus sylvestris* L.) stand: Evidences from continuous evapotranspiration and water table  
952 monitoring, *Agric. For. Meteorol.*, 148, 1419-1432, doi:10.1016/j.agrformet.2008.04.009,  
953 2008.

954 Wang, Y., Woodcock, C. E., Buermann, W., Stenberg, P., Voipio, P., Smolander, H., Häme,  
955 T., Tian, Y., Hu, J., Knyazikhin, Y. and Myneni, R. B.: Evaluation of the MODIS LAI  
956 algorithm at a coniferous forest site in Finland, *Remote Sens. Environ.*, 91, 114-127,  
957 doi:10.1016/j.rse.2004.02.007, 2004.

958 Westenbroeck, S. M., Kelson, V. A., Hunt, R. J. and Branbury, K.,R.: A modified  
959 Thornthwaite-Mather Soil-Water-Balance code for estimating groundwater recharge, USGS,  
960 Reston, Virginia, USA, 2010.

961 Wierenga, P., Hills, R. and Hudson, D.: The Las Cruces Trench Site: Characterization,  
962 Experimental Results, and One-Dimensional Flow Predictions, *Water Resour. Res.*, 27, 2695-  
963 2705, 1991.

964 Winter, T. C., Harvey, J. W., Franke, O. L. and Alley, W. M.: Ground water and surface  
965 water; a single resource, USGS, Denver, Colorado, 79 pp., 1998.

966 Xiao, C., Janssens, I. A., Yuste, J. and Ceulemans, R.: Variation of specific leaf area and  
967 upscaling to leaf area index in mature Scots pine, *Trees*, 20, 304-310, doi:10.1007/s00468-  
968 005-0039-x, 2006.

969 Zaitsoff, O.: Groundwater balance in the Oripää esker, National Board of Waters, Finland,  
970 Helsinki, 54-73 pp., 1984.

971 Zhou, Y.: A critical review of groundwater budget myth, safe yield and sustainability,  
972 *J. Hydrol.*, 370, 207-213, doi:10.1016/j.jhydrol.2009.03.009, 2009.

973

974

975

976

977

978

979

980

981 **Tables**

982 **Table 1.** Characteristics of the study site annual climate.

VARIABLE	MEAN	STD
Precipitation [mm]	591	91
Air Temperature [°C]	-0.7	1.1
Reference ET [mm]	426	26

983

984 **Table 2.** Randomly varied parameters, related equations and parameter ranges included in the  
 985 model runs. For full description of parameters and equations, see Jansson and Karlberg (2004).

Parameter	Part of the model affected	Range	Units	Source
LAI (leaf area index)	Transpiration	0 ... 3.5	-	Data, see section 2.1.1
h (canopy height)	Transpiration	5 ... 15	m	Data
$r_{lai}$ (increase in aerodynamic resistance with LAI)	Soil evaporation	25 ... 75	-	$\pm 50\%$ , estimate
$r_{\psi}$ (soil surface resistance control)	Soil evaporation	100...300	-	$\pm 50\%$ approximately to cover the surface resistance reported 150-1000 (Kelliher et al., 1998)
$\lambda_L$ (pore size distribution index)	Soil evaporation, lichen	0.4 ... 1	-	Estimate, to cover an easily drainable range of pressure-saturation curves
$\Psi_L$ (air entry)	Soil evaporation, lichen	1.5 ... 20	-	Estimate, to cover a easily drainable range of pressure-saturation curves
$\theta_L$ (porosity)	Soil evaporation, lichen	7.5...12.5	%	Data, lichen mean water retention $\pm SD$ from samples



$k_{mat,L}$ (matrix saturated hydraulic conductivity)	Soil evaporation, lichen	$5 \cdot 10^4 \dots 5 \cdot 10^7$	mm d <sup>-1</sup>	Estimate, high K values assumed
$t_{WD}$ (coefficient in the soil temperature response function)	Water uptake	10 ... 20	-	±50%, estimate
$\Psi_c$ (critical pressure head for water uptake reduction)	Water uptake	200...600	-	±50%, estimate
$k_{mat,S}$ (matrix saturated hydraulic conductivity)	<u>Soil</u> <u>Sediment</u> profile	1.707 $10^3 \dots 127.2 \cdot 10^3$	mm d <sup>-1</sup>	Data from <u>soil-sediment</u> sample particle size analysis
$k_{minuc}$ (minimum unsaturated hydraulic conductivity)	<u>Soil</u> <u>Sediment</u> profile	$1 \cdot 10^{-4} \dots 10^{-1}$	mm d <sup>-1</sup>	Estimate $k_{mat} \cdot 1E-5$
$\lambda_s$ (pore size distribution index)	<u>Soil</u> <u>Sediment</u> profile	0.4 ... 1	-	Range to cover measured pressure-saturation curves
$\Psi_s$ (air entry)	<u>Soil</u> <u>Sediment</u> profile	20 ... 40	-	Range to cover measured pressure-saturation curves
$\theta_s$ (porosity)	<u>Soil</u> <u>Sediment</u> profile	0.25...0.36	%	Range from soil samples
$\theta_r$ (residual water content)	<u>Soil</u> <u>Sediment</u> profile	0.01...0.05	%	Range to cover measured pressure-saturation curves

986  
987  
988  
989  
990  
991  
992

993

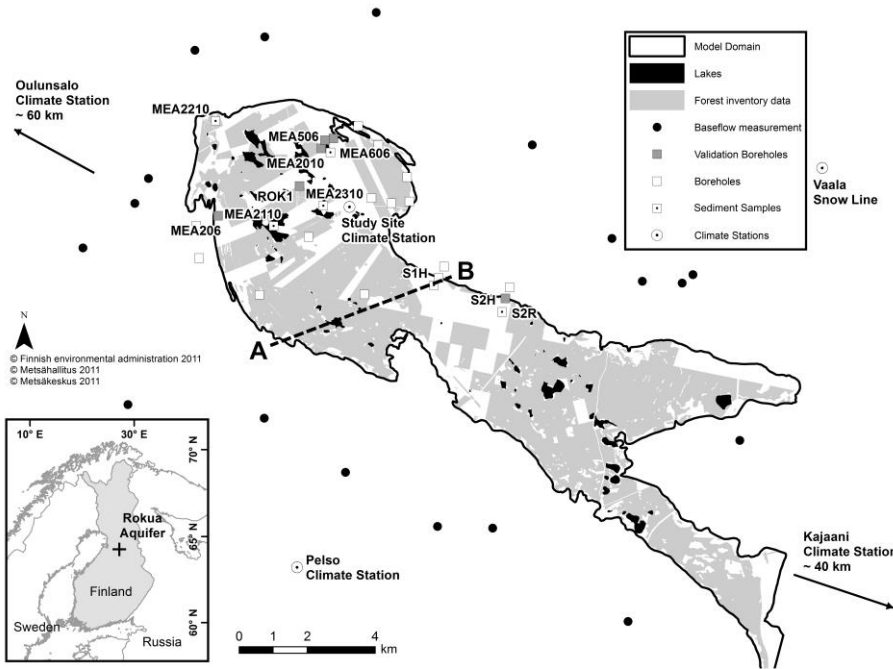
994 **Table 3.** Kendall correlation coefficient for simulation parameters and average annual sum of  
 995 simulation output variables. ET = evapotranspiration, E = evaporation, for other symbols see  
 996 Table 2.

Parameter	Total ET	Transpiration	Soil E	Snow E	Infiltration
LAI	0.59*	0.84*	-0.73*	-0.37*	0.18*
h	0.59*	0.84*	-0.73*	-0.37*	0.18*
$r_{\Psi}$	-0.11*	-0.03	-0.03	-0.61*	0.58*
$r_{lai}$	-0.13*	-0.02	-0.11*	0.03	-0.05
$\lambda_L$	-0.09*	-0.01	-0.11*	0.01	-0.03
$\Psi_L$	0.01	-0.04	0.11*	-0.04	0.06
$\theta_L$	0.06	0.03	0.01	-0.00	0.09*
$k_{mat,L}$	-0.01	0.02	-0.04	-0.00	-0.00
$k_{mat,S}$	-0.10*	-0.04	-0.07*	0.02	0.01
$k_{minuc}$	-0.10*	-0.04	-0.07*	0.02	0.01
$t_{WD}$	-0.05	-0.02	-0.03	-0.05	0.03
$\Psi_c$	0.18*	0.12*	-0.02	-0.04	0.05
$\lambda_s$	0.13*	0.06	0.06	-0.00	-0.23*
$\Psi_s$	-0.11*	-0.05	-0.04	-0.05	0.04
$\theta_s$	0.02	-0.01	0.03	0.10*	-0.18*
$\theta_r$	0.07*	0.05	-0.01	0.01	0.16*

997 \*Significant correlation,  $p < 0.05$

998

999 **Figures and captions**



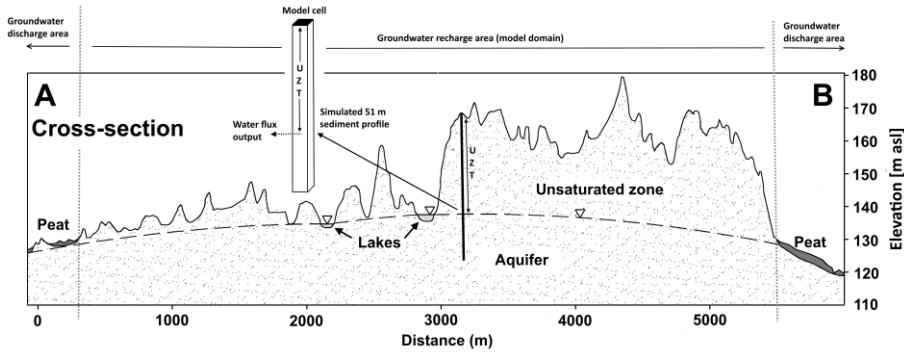
1000

1001 **Figure 1.** Recharge area of the Rokua esker aquifer. Boreholes in the area were used for model  
1002 validation and soil-sediment type characterization. Baseflow was measured from streams  
1003 originating outside the groundwater recharge area. Profile of cross-section A-B is presented in  
1004 Fig. 2.

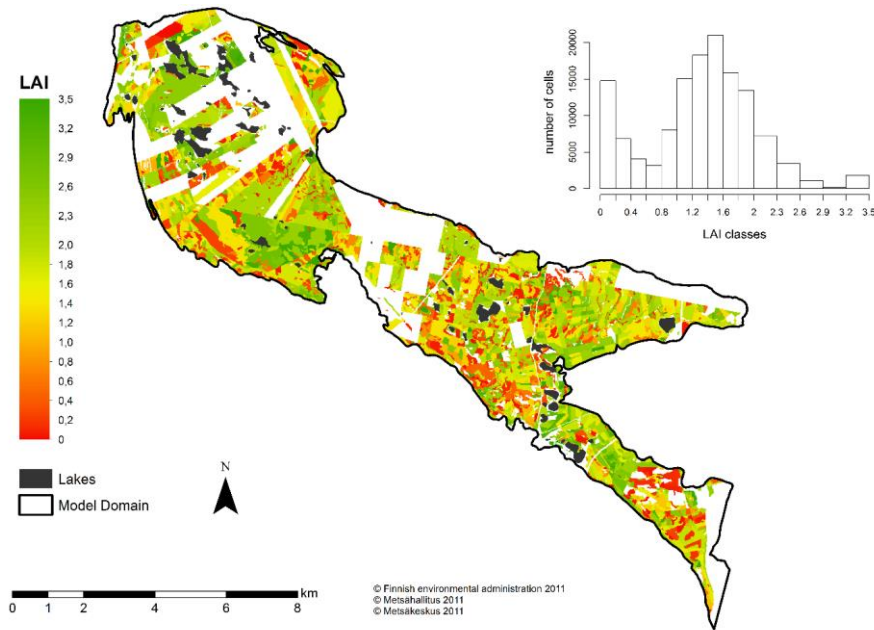
1005

1006

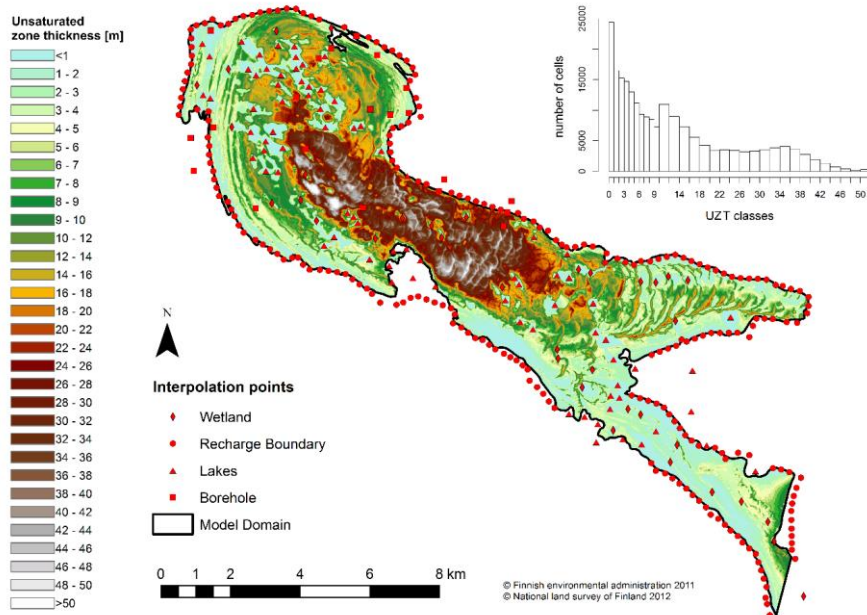
1007



1008  
 1009 **Figure 2.** Cross-section A-B (Fig. 1) to demonstrate the geometry of the unsaturated zone and  
 1010 the aquifer (vertical axes exaggerated). A simulated sediment soil profile is shown to give an  
 1011 example on how 1-D simulations are represented in the model domain, UZT represents the  
 1012 unsaturated zone thickness parameter.



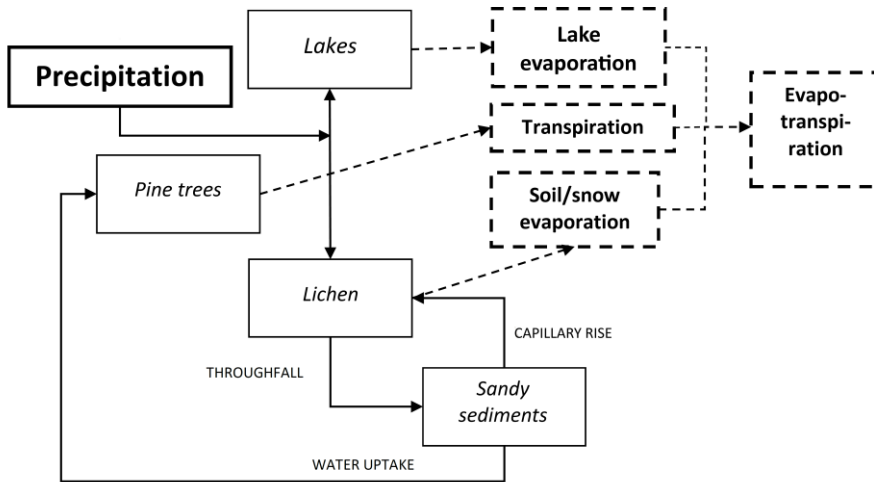
1013  
 1014 **Figure 3.** Spatial distribution of leaf area index (LAI) and a 20m x 20m cell-based histogram  
 1015 of LAI values. In areas where forestry inventory data were lacking, a weighted average value  
 1016 of 1.25 was used in simulations.



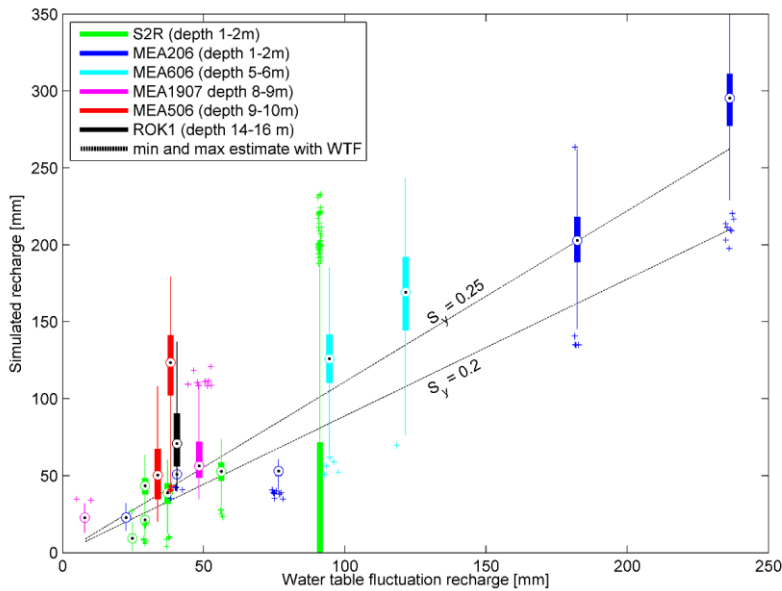
1017  
 1018 **Figure 4.** Estimated thickness of the unsaturated zone in the model area and interpolation points  
 1019 for estimation of water table elevation.

1020

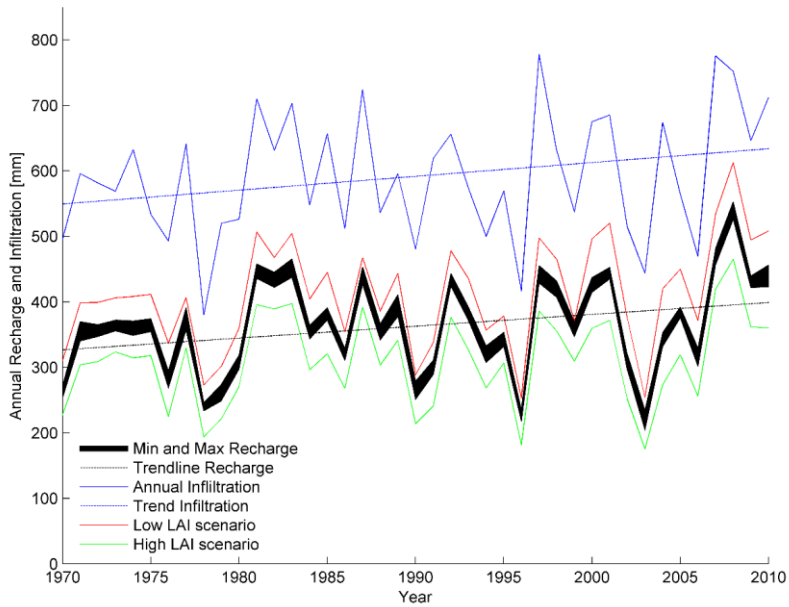
1021



1022  
 1023 **Figure 5.** Flow chart of different evaporation processes considered in the study. Total  
 1024 evapotranspiration comprises of soil evaporation from the topmost soil layer, i.e. the lichen  
 1025 matrix, snow evaporation from snow surface, transpiration through the vascular system of tree  
 1026 canopy and lake evaporation from free water surface.

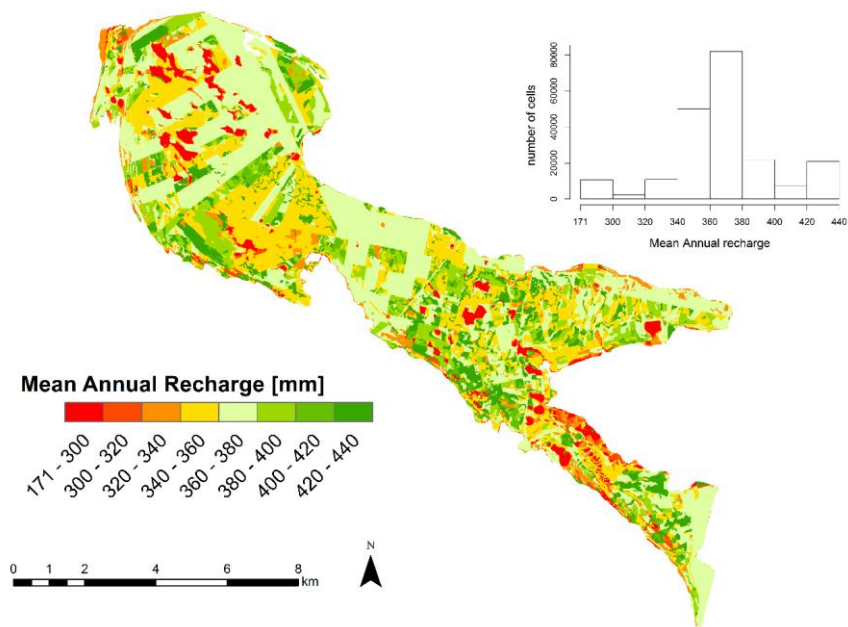


1027  
 1028 **Figure 6.** Assemblage of simulated recharge for individual recharge events, shown as boxplots  
 1029 where circles represent the median, bold lines 25-75<sup>th</sup> percentiles of the simulations, thin lines  
 1030 the remaining upper and lower 25<sup>th</sup> percentiles and crosses are outliers. The location of the  
 1031 boxplots on the x-axis is the WTF estimate for a given recharge event using a specific yield  
 1032 value of 0.225. The dashed lines indicate the uncertainty in the WTF estimates caused by the  
 1033 selection of specific yield. The two estimates would agree perfectly (given the uncertainty in  
 1034  $S_y$ ) if all simulations shown as boxplots fell between the dashed lines.

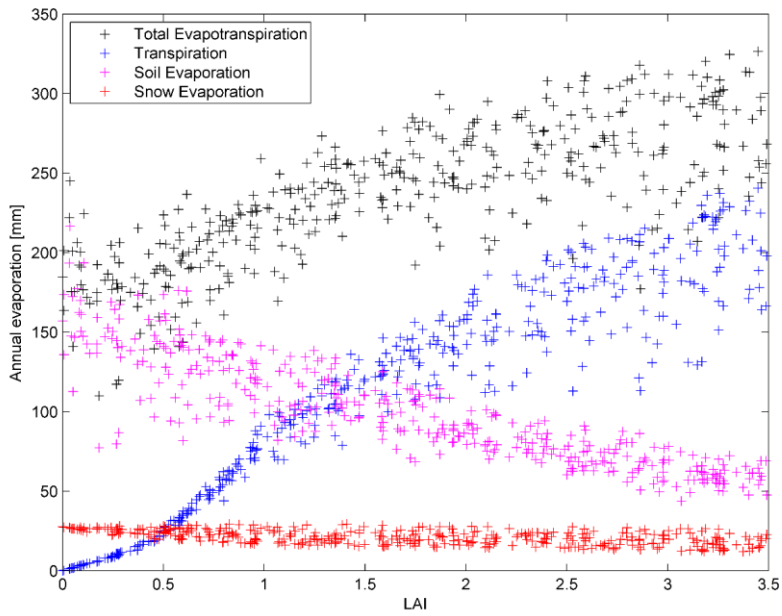


1035  
 1036 **Figure 7.** Annual recharge time series from simulations where the black area covers the  
 1037 minimum and maximum values for different recharge samples. The annual recharge pattern  
 1038 closely followed trends in infiltration. Effects of different land use management practices over  
 1039 time on annual recharge rates are shown as high and low leaf area index (LAI) scenarios.

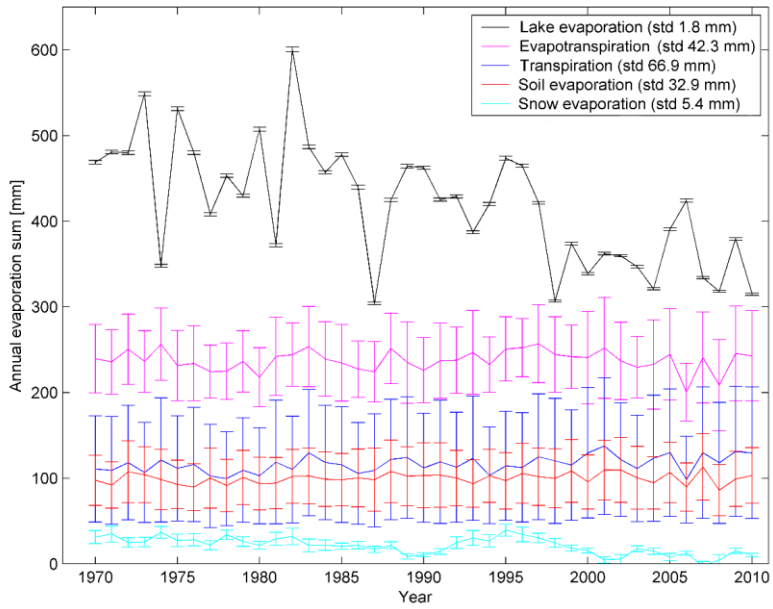




1040  
 1041 **Figure 8.** Spatial distribution of mean annual recharge, which was influenced mainly by the  
 1042 Scots pine canopy (LAI), the presence of lakes and, to some extent, areas with a shallow water  
 1043 table.



1044  
 1045 **Figure 9.** Example of scatter plots with the mean annual ET components are plotted as a  
 1046 function of the variable leaf area index (LAI), showing clear dependence of all ET components  
 1047 on LAI.



1048  
 1049 **Figure 10.** Values of different evapotranspiration (ET) components (mean and standard  
 1050 deviation) simulated for the study period.